



ELSEVIER

Available online at www.sciencedirect.com

SCIENCE @ DIRECT®

Physics Letters A 325 (2004) 430–434

PHYSICS LETTERS A

www.elsevier.com/locate/pla

Competition between the charge ordered and ferromagnetic states in $(\text{La,Nd})_{0.75}\text{Na}_{0.25}\text{MnO}_3$ manganites

Z.Q. Li^a, X.H. Zhang^a, J.S. Yu^a, X.J. Liu^a, X.D. Liu^{a,*}, H. Liu^a, P. Wu^a, H.L. Bai^a, C.Q. Sun^b, J.J. Lin^c, E.Y. Jiang^a

^a Institute of Advanced Materials Physics, School of Science, Tianjin University, Tianjin 300072, PR China

^b School of Electrical and Electronic Engineering, Block S2, Nanyang Technological University, Singapore 639798, Singapore

^c Institute of Physics, National Chiao Tung University, Hsinchu 300, Taiwan

Received 18 February 2004; accepted 5 April 2004

Communicated by J. Flouquet

Abstract

Structural, magnetic, and transport properties of $(\text{La}_{1-x}\text{Nd}_x)_{0.75}\text{Na}_{0.25}\text{MnO}_3$ ($0 \leq x \leq 1$) are studied. The system exhibits a rhombohedrally distorted perovskite structure for $x \leq 0.2$ and it convert to an orthorhombic structure for $x \geq 0.4$. Re-entrant ferromagnetic type charge ordering transitions are observed in the narrow bandwidth samples ($x \geq 0.6$), while charge ordering transition is not observed for these samples with rhombohedral structure. Combining with the published results related to the charge ordering transition, we argue that the rhombohedral structure likely favor double exchange interaction and suppress charge ordering interaction. The compounds show metal to insulator transitions except $\text{Nd}_{0.75}\text{Na}_{0.25}\text{MnO}_3$. The resistivity data above the metal to insulator transition temperature for the charge ordered sample are discussed in the frame work of variable-range hopping model.

© 2004 Elsevier B.V. All rights reserved.

PACS: 75.47.Lx; 75.47.Gk; 75.30.Kz

Keywords: Manganites; Colossal magnetoresistance; Charge-ordering; Phase separation

Recently there has been intensive interest in the properties of the rare-earth manganite perovskites $\text{R}_{1-x}\text{A}_x\text{MnO}_3$ where R is a rare-earth element such as La, Pr, Nd or Y, and A is one of a number of divalent ions including Sr, Ca, Ba and Pb. The reason is not only the colossal magnetoresistance (CMR) [1–3] that occurs in these systems, but also a rich variety of the

physical phenomena including intrinsically inhomogeneous ground states, phase separation, charge/orbital ordering [4,5]. Among these physical phenomena, investigations related to charge ordering (CO) are becoming increasingly popular and have to some extent diverted the interest in the rare earth manganates from CMR to phenomena related to CO. The properties of $\text{R}_{1-x}\text{A}_x\text{MnO}_3$ are sensitive to the hole doping level x and the average A-site radius $\langle r_A \rangle$ which determines the effective one-electron bandwidth (W) or, equivalently, Mn $3d$ e_g -electron transfer interac-

* Corresponding author.

E-mail address: xindianliu@yahoo.com (X.D. Liu).

tion (t). In the large W cases, the magnetic and electronic properties are mainly interpreted by the double exchange (DE) model [6], while in the reduced- W cases, the other instabilities competing with the DE interaction should be considered, such as the antiferromagnetic interaction between local t_{2g} spins, the collective Jahn–Teller effect [7–9], and the charge/orbital ordering [10].

Some manganites doped with univalent alkali metal cations also show CO phenomenon. $\text{Pr}_{1-x}\text{Na}_x\text{MnO}_3$ are charge-ordered antiferromagnets for $0.2 \leq x \leq 0.25$ below T_{CO} [11], and $\text{Nd}_{0.75}\text{Na}_{0.25}\text{MnO}_3$ undergoes a CO transition around 180 K [12]. However, the properties related to CO for the manganites doped with univalent alkali metal cations are not completely identical to that of manganites doped with divalent alkali earth cations. For example, the $\langle r_A \rangle$ of $\text{La}_{0.75}\text{Na}_{0.25}\text{MnO}_3$ is 1.22 Å, which is smaller than that of $\text{Nd}_{0.5}\text{Sr}_{0.5}\text{MnO}_3$ (1.24 Å). However, $\text{La}_{0.75}\text{Na}_{0.25}\text{MnO}_3$ do not show any charge ordering characters [13], while $\text{Nd}_{0.5}\text{Sr}_{0.5}\text{MnO}_3$ is a charge ordered antiferromagnet below 150 K [14,15]. Hence it is necessary to investigate the competition between the charge ordered and ferromagnetic states in manganites doped with univalent alkali metal cations. As mentioned above, $\text{La}_{0.75}\text{Na}_{0.25}\text{MnO}_3$ only undergoes a transition from ferromagnetic metal to paramagnetic insulator phase between 1.8 to 400 K [13], while a charge disordered paramagnetic insulator to charge ordered paramagnetic insulator transition occur at 180 K in $\text{Nd}_{0.75}\text{Na}_{0.25}\text{MnO}_3$ compound [14]. Therefore $(\text{La}_{1-x}\text{Nd}_x)_{0.75}\text{Na}_{0.25}\text{MnO}_3$ is the suitable system to investigate the competition between the ferromagnetic DE and CO interactions and resultant versatile metal–insulator (M-I) transition phenomena. In the present Letter, we systematically studied the structure magnetic and electronic transport properties of $(\text{La}_{1-x}\text{Nd}_x)_{0.75}\text{Na}_{0.25}\text{MnO}_3$ ($0 \leq x \leq 1$) compounds. The interactions between double exchange and charge ordering interaction varying with the bandwidth and crystalline structure are discussed.

$(\text{La}_{1-x}\text{Nd}_x)_{0.75}\text{Na}_{0.25}\text{MnO}_3$ ($x = 0, 0.1, 0.2, 0.4, 0.6, 0.8, 0.9, 1$) powder samples were synthesized via sol–gel route (Pechini process) [16] in order to obtain well mixed reagents. The powder was pressed into discs and sintered at 1373 K for 60 hours and then furnace cooled. The phase analysis of the samples was performed using a Rigaku X-ray diffractometer

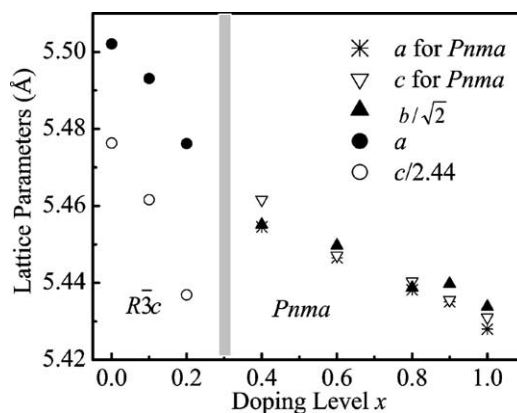


Fig. 1. Nd^{3+} concentration dependence of lattice constants at room temperature for $(\text{La}_{1-x}\text{Nd}_x)_{0.75}\text{Na}_{0.25}\text{MnO}_3$.

($D/\text{max-2500}\times$) with $\text{Cu } K_\alpha$ radiation at room temperature. The atomic fraction was determined by electron-probe microanalysis and inductive coupled plasma (ICP) emission spectroscopy, respectively. Both results indicate that the hole concentrations agree with the nominal concentrations within 1%. Magnetic properties were measured by using vibrating sample magnetometer (VSM). Resistivity measurements were carried out by four-probe method and electrical contacts were made with a silver conductive paint.

The X-ray patterns indicate that all samples are single phase and the diffractograms can be indexed based on a rhombohedrally or orthorhombically distorted perovskite structure. A Rietveld study [17] of the XRD data reveals the $R\bar{3}c$ symmetry (R phase) for $x \leq 0.2$ and the $Pnma$ symmetry (O phase) for $x \geq 0.4$. The corresponding lattice constants at room temperature are shown in Fig. 1. One can see that the lattice constants decrease with increasing x , no matter in R phase or O phase. Since the radius of La^{3+} is greater than that of Nd^{3+} and the rhombohedral structure most likely occurs in these manganites with large A-site radius such as $\text{La}_{1-x}\text{Sr}_x\text{MnO}_3$, $\text{La}_{1-x}\text{Ba}_x\text{MnO}_3$ and $\text{La}_{1-x}\text{Na}_x\text{MnO}_3$, it is reasonable to observe the reducing lattice constants with increasing x and the structure transition from R phase to O phase around $x = 0.3$.

Fig. 2 displays the temperature dependence of magnetization of the samples measured on zero field cooling (ZFC) model under 1000 Oe. For $x = 0$, the bandwidth is large which favor the DE interaction, and re-

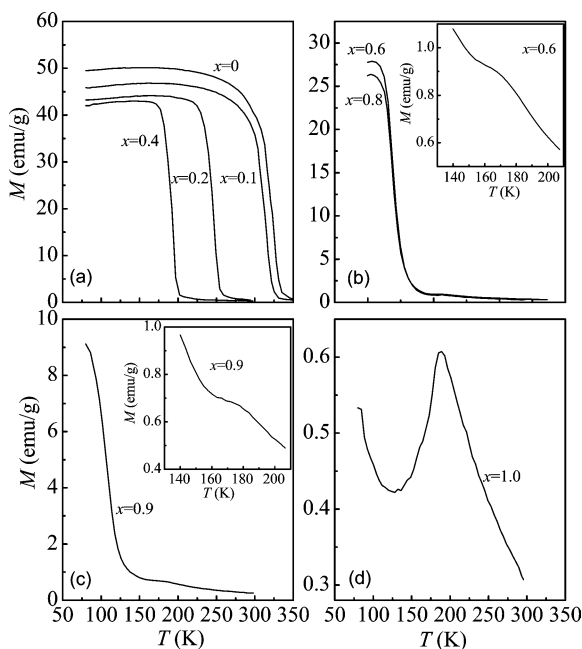


Fig. 2. Zero field cooled magnetization as a function of temperature for $(\text{La}_{1-x}\text{Nd}_x)_{0.75}\text{Na}_{0.25}\text{MnO}_3$ under a field of 1000 Oe, (a) for $x = 0, 0.1, 0.2, 0.4$; (b) for $x = 0.6$ and 0.8 ; (c) for $x = 0.9$; (d) for $x = 1$. The inset of (b) and (c) shows the detail information of the charge ordered range for $x = 0.6$ and 0.9 , respectively.

sult in the Curie temperature (T_C) as high as 325 K. When the Nd^{3+} is introduced, T_C reduce with decreasing bandwidth, i.e., with increasing Nd^{3+} doping level. For $x = 0.4$, the Curie temperature reduces to 192 K, but the DE interaction remains dominant and only ferromagnetic to paramagnetic phase transition is observed in the whole testing temperature range. When $x = 0.6$, the bandwidth is further reduced, and a charge ordering transition, characterize by an extra peak (or shoulder) [18,19] in the $M-T$ curve, occurs at 168 K. The charge ordering temperature (T_{CO}) was obtained from the minima in $|dM/dT|$ plot [18]. The behaviours for $x = 0.6, 0.8$ and 0.9 are similar. As depicted in Fig. 2, when the materials are cooled from room temperature a CO state first develops, then followed by FM state. This is generally called re-entrant FM behaviour [19]. For $x \geq 0.6$, T_{CO} increases with increasing of x , while T_C decreases with increasing of x . For the end member $\text{Nd}_{0.75}\text{Na}_{0.25}\text{MnO}_3$ whose $\langle r_A \rangle$ is the smallest, long range ferromagnetic interaction is not achieved yet even at 77, and only small

Table 1

Structural parameters, Curie temperature and charge ordering temperature for $(\text{La}_{1-x}\text{Nd}_x)_{0.75}\text{Na}_{0.25}\text{MnO}_3$ ($0 \leq x \leq 1$)

Nd^{3+} doping level	$\langle r_A \rangle$ (\AA)	σ^2 (\AA^2)	T_C (K)	T_{CO} (K)
1.0	1.182	0.00112	–	180
0.9	1.186	0.00115	109	176
0.8	1.190	0.00116	112	172
0.6	1.198	0.00109	115	168
0.4	1.206	0.00089	192	–
0.2	1.214	0.00056	246	–
0.1	1.218	0.00035	315	–
0	1.222	0.00011	325	–

fraction of ferromagnetic components is found below 130 K [12]. This indicates that the charge ordering phase is dominant in the narrow bandwidth compound $\text{Nd}_{0.75}\text{Na}_{0.25}\text{MnO}_3$. The $\langle r_A \rangle$ of $\text{Nd}_{0.75}\text{Na}_{0.25}\text{MnO}_3$ is 1.182 \AA , which is exactly identical to that of $\text{La}_{0.2}\text{Nd}_{0.3}\text{Ca}_{0.5}\text{MnO}_3$. But the T_{CO} of the former (180 K) is much less than that of the latter (237 K) [19]. This may caused by the larger size mismatch of the A-site cations σ^2 of the former, here $\sigma^2 = \sum x_i r_i^2 - \langle r_A \rangle^2$, where x_i is the fractional occupancy of A ions and r_i is the corresponding ionic radii. For $(\text{La}_{1-x}\text{Nd}_x)_{0.75}\text{MnO}_3$ series, the average A-site radius, size mismatch of the A-site cations, CO temperature and Curie temperature are listed in Table 1. Form this table, one can see that the magnitudes of $\langle r_A \rangle$ for these charge ordered manganites are exactly in the range 1.17–1.20 \AA , which is identical to that re-entrant type manganites doped with divalent alkali earth cations. The values of σ^2 for the re-entrant type manganites studied by Rao et al. are about one-tenth of that for our samples, hence the relative lower T_{CO} of $(\text{La}_{1-x}\text{Nd}_x)_{0.75}\text{Na}_{0.25}\text{MnO}_3$ ($x \geq 0.6$) may related to the larger size mismatch of the A-site cations. On the other hand, although both the $\langle r_A \rangle$ and σ^2 of the $x \leq 0.2$ samples are less than that of $\text{Nd}_{0.3}\text{La}_{0.2}\text{Sr}_{0.5}\text{MnO}_3$ ($\langle r_A \rangle = 1.25$ \AA and $T_{CO} = 120$ K) [20], which favor to the CO phase, CO transition is not observed in these samples. It should note that the $x \leq 0.2$ samples are rhombohedral structure, to our knowledge, none of those charge ordered manganites no matter doped with divalent alkali earth cations or univalent alkali metal cations, such as $\text{Nd}_{1-x}\text{Ca}_x\text{MnO}_3$ ($0.3 \leq x < 0.8$) [21], $\text{Nd}_{1-x}\text{Sr}_x\text{MnO}_3$ ($0.48 < x < 0.52$) [14], $\text{Pr}_{1-x}\text{Ca}_x\text{MnO}_3$ ($0.3 \leq x < 0.7$) [22–24], $\text{La}_{1-x}\text{Ca}_x\text{MnO}_3$ ($x \geq 0.5$) [25], $(\text{Nd}_{1-x}\text{La}_x)_{0.5}\text{Sr}_{0.5}$

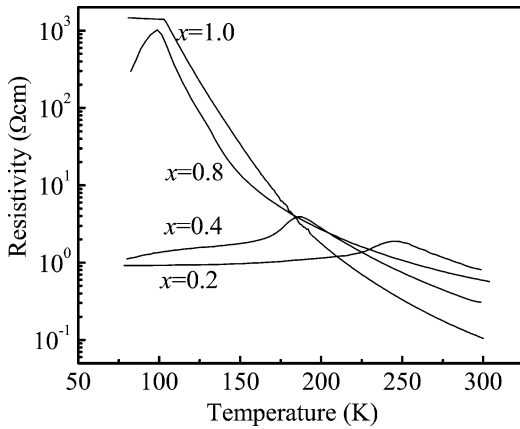


Fig. 3. Temperature variation of the resistivity of $(\text{La}_{1-x}\text{Nd}_x)_{0.75}\text{Na}_{0.25}\text{MnO}_3$ ($x = 1, 0.8, 0.4, 0.2$) at zero field.

MnO_3 ($x \leq 0.4$) [20], $(\text{Nd,Sm})_{0.5}\text{Sr}_{0.5}\text{MnO}_3$ [26] and $\text{Pr}_{1-x}\text{Na}_x\text{MnO}_3$ ($0.2 \leq x \leq 0.25$) [11], etc., has rhombohedral structure. Hence we argue that the rhombohedral structure likely favor double exchange interaction and suppress charge ordering interaction.

The temperature dependence of the resistivity of $(\text{La}_{1-x}\text{Nd}_x)_{0.75}\text{Na}_{0.25}\text{MnO}_3$ is displayed in Fig. 3. For clarify, only the figures of $x = 1, 0.8, 0.4$ and 0.2 are given. M-I transitions are observed for all other samples except $\text{Nd}_{0.75}\text{Na}_{0.25}\text{MnO}_3$. The transition temperatures are coincident with corresponding Curie temperatures, i.e., the metallic states of the samples are ferromagnetic.

Three typical models are generally used to explain the conduction mechanism above the M-I transition temperature. These models are proposed in terms of conventional thermal activation (TA), small polaron hopping (SPH) [27], and variable-range hopping (VRH) [28], respectively. Each predicts a different temperature dependence of resistivity as $\rho = A \exp(E_\alpha/k_B T)$ (TA), $\rho = BT \exp(E_\alpha/k_B T)$ (SPH) and $\rho = \rho_0 \exp(T_0/T)^{1/4}$ (VRH), where k_B is Boltzmann constant and E_α is the activation energy. For the charge ordered samples, the resistivity data above T_C (above 110 K for $\text{Nd}_{0.75}\text{Na}_{0.25}\text{MnO}_3$) are fitted using the three models, respectively. Since the fitting results for the charge ordered samples are similar, only the results of $\text{Nd}_{0.75}\text{Na}_{0.25}\text{MnO}_3$ are presented and discussed here. Fig. 4 displays the $\ln \rho$ versus $1/T^{1/4}$ for $T > 110$ K. Surprisingly, these data are roughly in two distinct straight lines with different slopes and

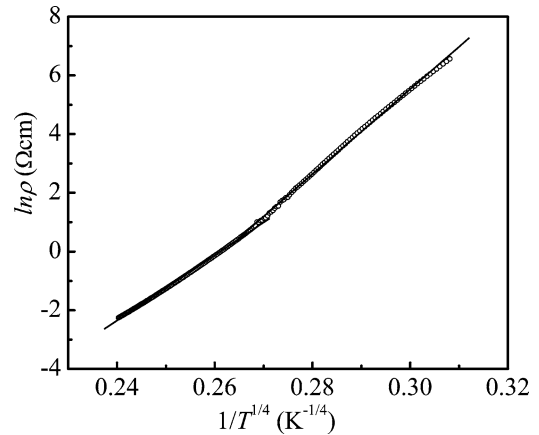


Fig. 4. $\ln \rho$ versus $1/T^{1/4}$ for $\text{Nd}_{0.75}\text{Na}_{0.25}\text{MnO}_3$ above 110 K. The solid lines are fits to VRH model with different localization length.

the crossing section for the two straight lines is around 190 K ($1/T^{1/4} = 0.269$) which is close to T_{CO} . We fit the two lines using least square root method and the results are also shown in Fig. 4 (solid lines). Neither of the TA and SPH model can well reproduce the experimental data even if the data are separated into two parts. Hence the resistivity follows Mott's VRH model above 110 K for $\text{Nd}_{0.75}\text{Na}_{0.25}\text{MnO}_3$. In the VRH model, the parameter T_0 is related to localization length L by the expression $k_B T_0 = 18/[L^3 N(E)]$, where $N(E)$ is the electronic density of states. The fitting results indicate that T_0 is equal to 4.3718×10^8 K for $T < 190$ K and 1.52303×10^8 K for $T > 190$ K, respectively. Therefore the localization length for $T < 190$ K is less than that for $T > 190$ K, which indicate the carriers become more localized below 190 K. Since the CO transition temperature is 180 K and CO generally makes the carriers more localized [4,10], the change of slope in $\ln \rho$ versus $1/T^{1/4}$ curve around 190 K originates from CO transition.

In summary, we systematically studied the structure, magnetic and electronic transport properties of $(\text{La}_{1-x}\text{Nd}_x)_{0.75}\text{Na}_{0.25}\text{MnO}_3$ ($0 \leq x \leq 1$) systems. $\text{La}_{0.75}\text{Na}_{0.25}\text{MnO}_3$ is a ferromagnetic metal with rhombohedral structure below Curie temperature, and it undergoes a ferromagnetic metal to paramagnetic insulator transition at 325 K. The system converts to an orthorhombically distorted perovskite structure for $x \geq 0.4$. Re-entrant ferromagnetic type charge ordering transitions are observed in the narrow bandwidth

samples whose $\langle r_A \rangle$ is less than 1.20 \AA . T_C increases with increasing bandwidth while T_{CO} decreases with increasing bandwidth. Combining with the published results related to the charge ordering transition, we argue that the rhombohedral structure likely favor double exchange interaction and suppress charge ordering interaction in manganites. M-I transitions are observed for all other samples except $\text{Nd}_{0.75}\text{Na}_{0.25}\text{MnO}_3$. The resistivity data above the metal to insulator transition temperature for the charge ordered sample follow VRH model, what is more, the localization length below T_{CO} is less than that above T_{CO} , which indicates that the CO makes charge carries more localized.

Acknowledgements

This work is financial supported by Natural Science Foundation of Tianjin City and National Natural Science Foundation of China (Contract No. 50172033).

References

- [1] R. von Helmolt, J. Wecker, B. Holzapfel, L. Schultz, K. Samwer, *Phys. Rev. Lett.* 71 (1993) 2331.
- [2] K. Chahara, T. Ohno, M. Kasai, Y. Kozono, *Appl. Phys. Lett.* 63 (1993) 1990.
- [3] S. Jin, T.H. Tiefel, M. McCormack, R.A. Fastnacht, R. Ramesh, L.H. Chen, *Science* 264 (1994) 413.
- [4] E. Dagotto, T. Hotta, A. Moreo, *Phys. Rep.* 344 (2001) 1.
- [5] M.M. Salamon, M. Jaime, *Rev. Mod. Phys.* 73 (2001) 583.
- [6] C. Zener, *Phys. Rev.* 82 (1951) 403.
- [7] A.J. Millis, P.B. Littlewood, B.I. Shraiman, *Phys. Rev. Lett.* 75 (1995) 3910.
- [8] A.J. Millis, B.I. Shraiman, R. Mueller, *Phys. Rev. Lett.* 77 (1996) 175.
- [9] H. Röder, J. Zang, A.R. Bishop, *Phys. Rev. Lett.* 76 (1996) 1356.
- [10] C.N.R. Rao, A. Arulraj, A.K. Cheetham, B. Raveau, *J. Phys.: Condens. Matter* 12 (2000) R83.
- [11] J. Hejtmanek, Z. Jirák, J. Šebek, A. Strejc, M. Hervieu, *J. Appl. Phys.* 89 (2001) 7413.
- [12] X.J. Liu, E.Y. Jiang, Z.Q. Li, B.L. Li, W.R. Li, A. Yu, H.L. Bai, *Physica B* 348 (2004) 146.
- [13] S. Roy, Y.Q. Guo, S. Venkatesh, N. Ali, *J. Phys.: Condens. Matter* 13 (2001) 9547.
- [14] R. Kajimoto, H. Yoshizawa, H. Kawano, H. Kuwahara, Y. Tokura, K. Ohoyama, M. Ohashi, *Phys. Rev. B* 60 (1999) R9506.
- [15] C. Ritter, R. Mahendiran, M.R. Ibarra, L. Morellon, A. Maignan, B. Raveau, C.N.R. Rao, *Phys. Rev. B* 61 (1999) R9229.
- [16] Z.Q. Li, E.Y. Jiang, D.X. Zhang, D.L. Hou, W.C. Li, H.L. Bai, *Phys. Lett. A* 277 (2000) 56.
- [17] R.A. Young, A. Sakthivel, T.S. Moss, C.O. Paiva-Aantos, *J. Appl. Crystallogr.* 28 (1995) 366.
- [18] P.V. Vanitha, P.N. Santhosh, R.S. Singh, C.N.R. Rao, J.P. Attfield, *Phys. Rev. B* 59 (1999) 13539.
- [19] P.V. Vanitha, C.N.R. Rao, *J. Phys.: Condens. Matter* 13 (2001) 11707.
- [20] Y. Moritomo, H. Kuwahara, Y. Tomioka, Y. Tokura, *Phys. Rev. B* 55 (1997) 7549.
- [21] K. Liu, X.W. Wu, K.H. Ahn, T. Sulchek, C.L. Chien, *Phys. Rev. B* 54 (1996) 3007.
- [22] E. Pollert, S. Krupicka, E. Kuzmicova, *J. Phys. Chem. Solids* 43 (1982) 1137.
- [23] Z. Jirák, S. Krupička, V. Nekvasil, E. Pollert, G. Villeneuve, F. Zounová, *J. Magn. Magn. Mater.* 15–18 (1980) 519.
- [24] Z. Jirák, S. Krupička, Z. Šimšá, M. Dlouhá, S. Vratislav, *J. Magn. Magn. Mater.* 53 (1985) 153.
- [25] P. Schiffer, A.P. Ramirez, W. Bao, S.-W. Cheong, *Phys. Rev. Lett.* 75 (1995) 3336.
- [26] H. Kuwahara, Y. Moritomo, Y. Tomioka, A. Asamitsu, M. Kasai, R. Kumai, Y. Tokura, *Phys. Rev. B* 56 (1997) 9386.
- [27] D. Emin, T. Holstein, *Phys. Rev. B* 13 (1976) 647.
- [28] N.F. Mott, E.A. Davies, *Electronic Processes in Noncrystalline Materials*, Oxford Univ. Press, Oxford, 1971.